

Full paper

Novel sweep-type triboelectric nanogenerator utilizing single freewheel for random triggering motion energy harvesting and driver habits monitoring

Zhijie Xie^{a,1}, Zhenghui Zeng^{a,1}, Yuqi Wang^{b,c,1}, Weixiong Yang^{b,c}, Yuhong Xu^{b,c}, Xiaohui Lu^b, Tinghai Cheng^{b,c,**}, Hongwei Zhao^{d,***}, Zhong Lin Wang^{c,e,*}

^a School of Mechatronics Engineering, Harbin Institute of Technology, Harbin, Heilongjiang, 150001, China

^b School of Mechatronic Engineering, Changchun University of Technology, Changchun, Jilin, 130012, China

^c Beijing Institute of Nanoenergy and Nanosystems, Chinese Academy of Sciences, Beijing, 100083, China

^d School of Mechanical and Aerospace Engineering, Jilin University, Changchun, Jilin, 130022, China

^e School of Materials Science and Engineering, Georgia Institute of Technology, Atlanta, GA, 30332-0245, United States



ARTICLE INFO

Keywords:

Triboelectric nanogenerators
Single freewheel
Random triggering motion
Harvesting mechanical energy
Driver habits monitoring

ABSTRACT

Traffic safety has always been a social concern, and driver habits directly affect traffic safety. Therefore it is significant to monitor driver habits. The pedal is the core operating device in the process of driving, so increasingly importance has been attached to the step movement of driver. The triboelectric nanogenerators (TENGs) performs well in harvesting the energy of random triggering motion and reflecting the characteristics of random triggering motion. This reports a novel sweep-type triboelectric nanogenerator (ST-TENG), which consists of a push rod, shells, two flywheels and a single freewheel. ST-TENG can harvest the energy of random triggering motion and monitor driver habits. Experiments show that the ST-TENG can generate the open-circuit voltage is 400 V and the short-circuit current is 15 μ A, and it is found that ST-TENG data could be exploited to reflect road conditions and driver habits. And ST-TENG has the potential to popularize intelligent driving systems.

1. Introduction

In recent years, with the gradual increase in car ownership, the number of deaths caused by traffic accidents has soared. Every year, around 4.5 million people die in traffic accidents and about 650 million people are injured or disabled in traffic accidents [1]. Poor driver habits and impulsive driving are the main causes of traffic accidents [2–6], and the pedal is an important component in the driving process. Signals generated by the driver stepping on a pedal can reflect driving habits [7]. Because of the randomness of road conditions, the pedal movement is triggered randomly, so the monitor device needs to be able to respond to random trigger motion. There are currently a number of devices that can monitor random trigger motion characteristics [8].

TENGs were first proposed by Wang's group in 2012 [9,10] and have increasingly received attention around the world. TENGs based on the coupling principle of triboelectrification and electrostatic induction

convert mechanical energy into electrical energy and generate characteristic signals [11–15]. TENGs are characterized by low cost and simple manufacturing. TENGs harvest different types of mechanical energy, such as vibrations [16,17], human motion [18,19], wind [20,21], rain drops [22] and water flow [23], from the environment. TENGs can even harvest large-scale blue energy through the connection of multiple units into a network [24,25]. Besides, TENGs can also be used as sensors [26–29]. In particular, TENGs can respond to random motion characteristics [30,31], particularly in the field of cars [32,33]. The stee ring wheel and pedals are important operating parts in the driving process, and can monitor driver habits.

In this paper a novel sweep-type triboelectric nanogenerator (ST-TENG) was designed that can harvest the energy of random triggering motion and monitor driver habits. The ST-TENG mainly includes a push rod, shells, two flywheels and a single freewheel. On the basis of the one-way transmission of the single freewheel and the energy storage of the

* Corresponding author. Beijing Institute of Nanoenergy and Nanosystems, Chinese Academy of Sciences, Beijing, 100083, China.

** Corresponding author. School of Mechatronic Engineering, Changchun University of Technology, Changchun, Jilin, 130012, China.

*** Corresponding author. School of Mechanical and Aerospace Engineering, Jilin University, Changchun, Jilin, 130022, China.

E-mail addresses: cth@ccut.edu.cn (T. Cheng), hwzhao@jlu.edu.cn (H. Zhao), zhong.wang@mse.gatech.edu (Z.L. Wang).

¹ These authors contributed equally to this work.

flywheel, the ST-TENG can transform the random triggering motion into continuous rotary motion. When the random triggering motion is applied to the push rod, the push rod and single freewheel transform the triggering motion into rotation motion of the shaft. The flywheel is driven by a rotating shaft to store energy and can rotate continuously. Triboelectric material is arranged around the flywheel, which can slide relative to the electrodes on the shells, and the electrodes thus generate electrical energy according to the coupling principle of triboelectrification and electrostatic induction. The performance of the ST-TENG under different settings is tested. In ST-TENG performance testing, the maximum running time of the ST-TENG is 6 s under a single trigger. Under optimal parameters, the ST-TENG can generate the open-circuit voltage is 400 V and the short-circuit current is 15 μ A. Each generating unit (TENG 1) can produce electric energy output of 1.7 mJ. The ST-TENG easily illuminates more than 500 light-emitting diodes (LEDs) via a rectifier. Through paralleling rectifiers and commercial capacitors, the ST-TENG can operate a commercial thermometer. The ST-TENG also monitors driver habits, and may analyze road conditions. The ST-TENG is vital to micro-energy capture and sensing and at the same time, as well as in the monitoring of driver habits, intelligent driving, and traffic safety. By cooperating with the machine learning and on-board intelligent driving system, transmitting real-time data to a cellphone, data of each driver can be used for future connected vehicles [34].

2. Results and discussion

2.1. Structural design and operation principle

This reports a novel sweep-type triboelectric nanogenerator (ST-TENG), as sketched in Fig. 1a. Fig. 1b shows the details of the energy-generating part (TENG 1), which comprises flexible fluorinated ethylene propylene (FEP) films (Fig. 1c) and copper electrodes. Fig. 1d shows the assembled ST-TENG with dimensions of 125 mm (length) \times 95 mm (width) \times 95 mm (height). The ST-TENG comprises four parts, namely a push rod, shells, two flywheels and a single freewheel, as shown in Fig. 1e. Fig. 1f shows the flywheel component.

The push rod is inserted in the shell, and receives random triggering motion. The random triggering motion is converted into continuous rotational motion by the push rod and single freewheel. Five flexible FEP films with a width of 30 mm are uniformly placed on the outer wall of a

flywheel. Ten copper electrodes with a width of 25 mm and a length of 30 mm are evenly distributed on the inner wall of a shell. Such a design ensures maximum space utilization, and the flexible FEP films do not interfere with each other. One end of each flexible FEP film is inserted into the flywheel and the other end is in contact with the copper electrode on the inner wall of the shells. Therefore, the flexible FEP film is able to rotate with the flywheel and slides against the copper electrode to generate electricity. When the random triggering motion disappears, the push rod returns to its initial position using the restoring force of the return spring. The single freewheel does not transfer force in the return of the push rod. To harvest more energy, mass plates of 44 g can be added to the flywheel, changing the mass of the flywheel to improve energy storage. Detailed experimental tests are reported later in the article. The push rod is triggered by random motion, and the ST-TENG therefore repeats the above process to harvest energy from the motion.

Fig. 2a shows the operation principle of the ST-TENG. As explained previously, a flexible FEP film makes contact with the copper electrode on the inner wall of the shells. When the flywheel is at its initial position, as illustrated in Fig. 2a i, the flexible FEP film is fully aligned with copper-1. Under the triboelectric effect, electrons transfer from copper-1 to the flexible FEP film because the electronegativity of the flexible FEP film is greater than that of copper in the triboelectric series [35]. At the same time, copper-1 has the same positive charge. In this state, that the positive and negative charges are equal, no current is generated in the external circuit between copper-1 and copper-2 because the positive and negative charges are equal. As the flywheel rotates, the flexible FEP film begins to slide relative to copper-1 and makes contact with copper-2 gradually. According to the principle of electrostatic induction, a potential difference drives the positive charge from copper-1 to copper-2, as shown in Fig. 2a ii. Until the flexible FEP film completely overlaps with copper-2, all positive charges are transferred to copper-2 as shown in Fig. 2a iii. The flywheel keeps rotating, and when the flexible FEP film makes contact with copper-1 again, positive charge flows from copper-2 to copper-1, as shown in Fig. 2a iv. The flexible FEP film then overlaps again with copper-1, as shown in Fig. 2a i. In this cycle, alternating currents are generated in the circuit. Therefore, ST-TENG receives a random triggering motion, the flywheel continues to rotate, resulting in alternating current between external circuits.

In order to prove the feasibility of this structure, the potential distribution between two adjacent electrodes was simulated using COMSOL software (Fig. 2b). The potential contour clearly shows that the potential

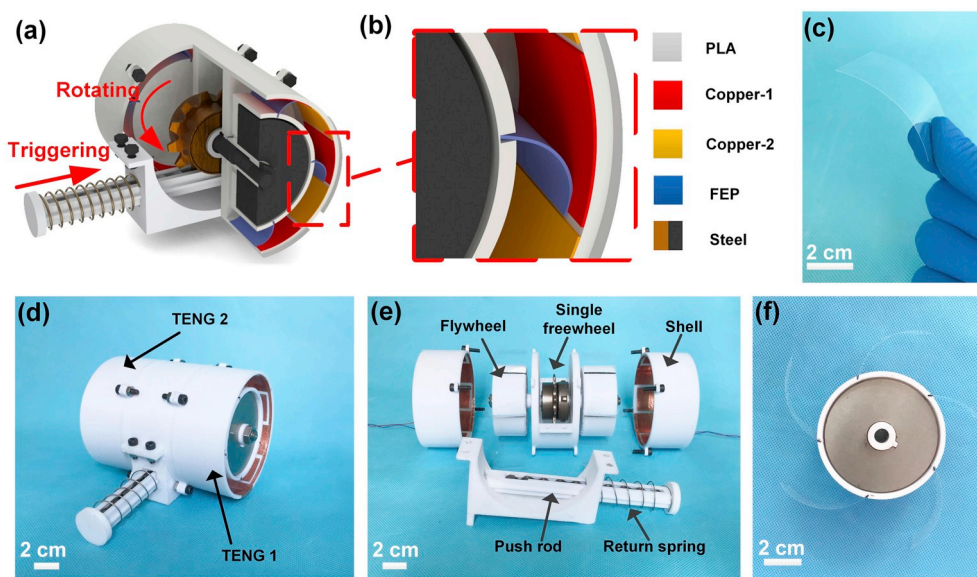


Fig. 1. Structural design of the novel sweep-type triboelectric nanogenerator (ST-TENG): (a) Schematic diagram of the ST-TENG, (b) enlarged image of the energy-generating part (TENG 1), (c) flexible FEP film as friction material, (d) photograph of assembly, (e) components of the ST-TENG and (f) flywheel (scale bar: 2 cm).

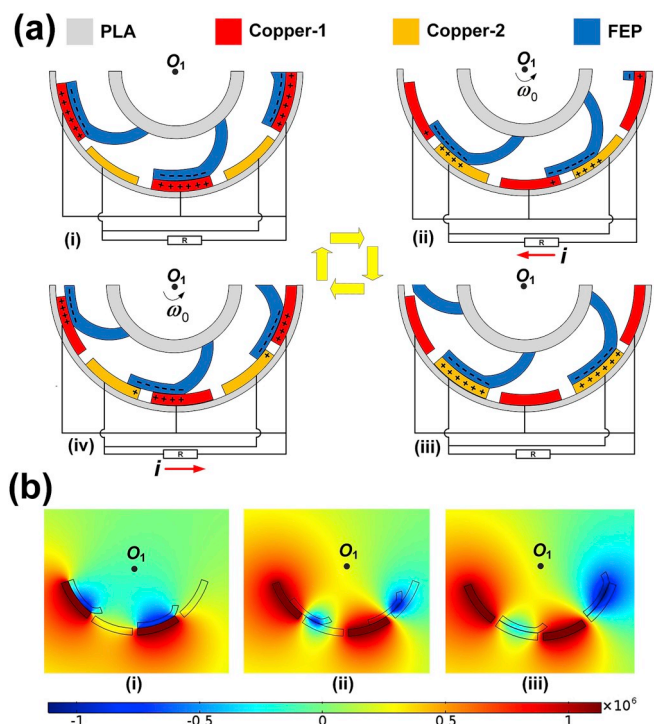


Fig. 2. Operation principle of the ST-TENG: (a) Schematic diagram of the operation principle of the ST-TENG and (b) simulation of the ST-TENG in three states.

difference between the two types of electrodes, which drives the current flowing in the external circuit.

2.2. Performance

The flexible FEP film parameters and flywheel mass can affect ST-TENG output [36]. The ability of the ST-TENG to capture randomly triggered movements and how to achieve greater energy output are investigated, as shown in Figs. S1, S2, S3, S4 and S5. This obtains parameters for optimum energy output of the ST-TENG, flywheel mass of

1.326 kg, an angle of the flexible FEP film of 60° and a length of the flexible FEP film of 55 mm. Fig. 3 presents the performance of the ST-TENG for a triggering speed of 1.2 m/s, flywheel mass of 1.326 kg, angle of the flexible FEP film of 60° and length of a flexible FEP film of 55 mm.

Fig. 3a and b shows that the performance of TENG 1 and TENG 2 placed in parallel is 1.6 times that of TENG 1. As the speed of the flywheel slows down from fast, the centrifugal force on the flexible film changes from large to small, resulting in a slight change in the contact state between the electrode and the flexible film, and a slight fluctuation in the voltage. Fig. 3c–g presents results for TENG 1 and TENG 2 placed in parallel. Fig. 3c shows that the ST-TENG has the highest output power (2.4 mW) when the load is 70 MΩ. Fig. 3d shows the time taken for different capacitors to charge from 0 to 15 V. Fig. 3e shows that for a triggering speed of 1.2 m/s, a single triggering can light up 500 LEDs for 6 s (Details are presented in Supporting Movie S1). Fig. 3f, the stepper motor triggers every 3.5 s, when the capacitive voltage can reach 1.5 V, switching on the temperature and humidity sensor and finally making it work steadily. Fig. 3g presents powering a thermometer by ST-TENG experimental system (Details are presented in Supporting Movie S2).

Supplementary data related to this article can be found at <https://doi.org/10.1016/j.nanoen.2019.104360>.

3. Driver habits monitoring

The sweep-type triboelectric nanogenerator (ST-TENG) can effectively reflect the trigger motion characteristics. This study adopted the manual gear driving simulator shown in Fig. 4, details are presented in Supporting Movie S3. Fig. 4a shows the simulation installation of ST-TENG. Fig. 4b i shows the experimental system of the driver during operation. Fig. 4b ii shows the ST-TENG mounted under the pedals of the car. The ST-TENG parameters are a flywheel mass of 1.326 kg, angle of the flexible FEP film of 60° and length of the flexible FEP film of 55 mm. Driver habits (Fig. 4c i) and the road conditions (Fig. 4c ii) can be reflected by analyzing the original signals.

Supplementary data related to this article can be found at <https://doi.org/10.1016/j.nanoen.2019.104360>.

Fig. 5 shows the steps for processing ST-TENG output signal. Here, Driver A is taken as an example, a detailed study was carried out subsequently. The original signal of the Driver A is shown in Fig. 5a. Fig. 5b presents the times that Driver A stepped on the accelerator and brake

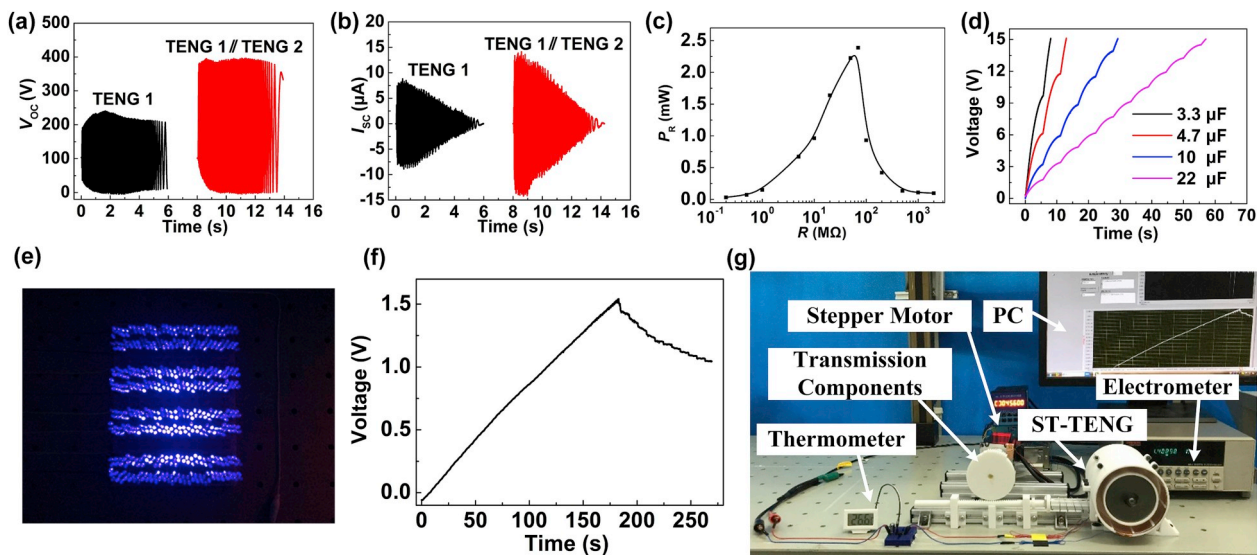


Fig. 3. Open-circuit voltage (a) and short-circuit current (b) of TENG 1 and TENG 1 and TENG 2 in parallel. (c) Instantaneous power of the ST-TENG under different loads. (d) Charging time of different types of capacitor from 0 to 15 V. (e) Lighting up of 500 LEDs in parallel. (f) Voltage curve for powering a small commercial thermometer. (g) Powering a thermometer by ST-TENG experimental system.

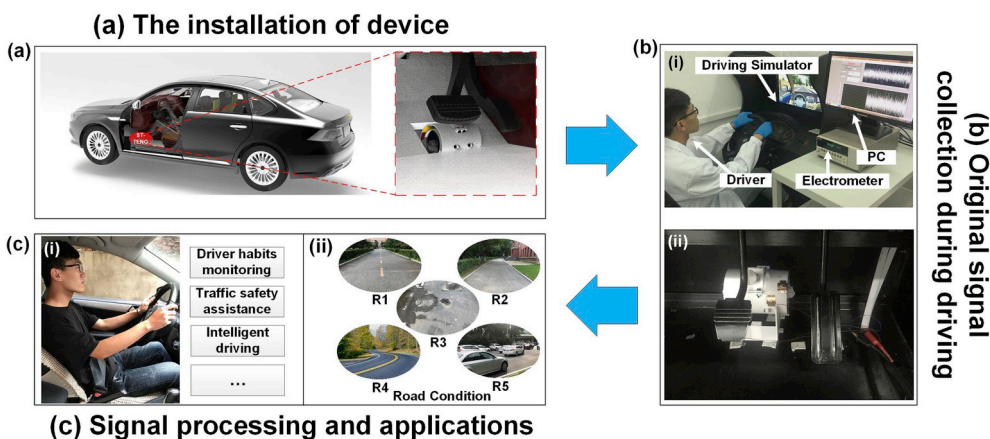


Fig. 4. Monitoring of driver habits: (a) Simulation installation of ST-TENG; (b) experimental system; (c) application field and road condition.

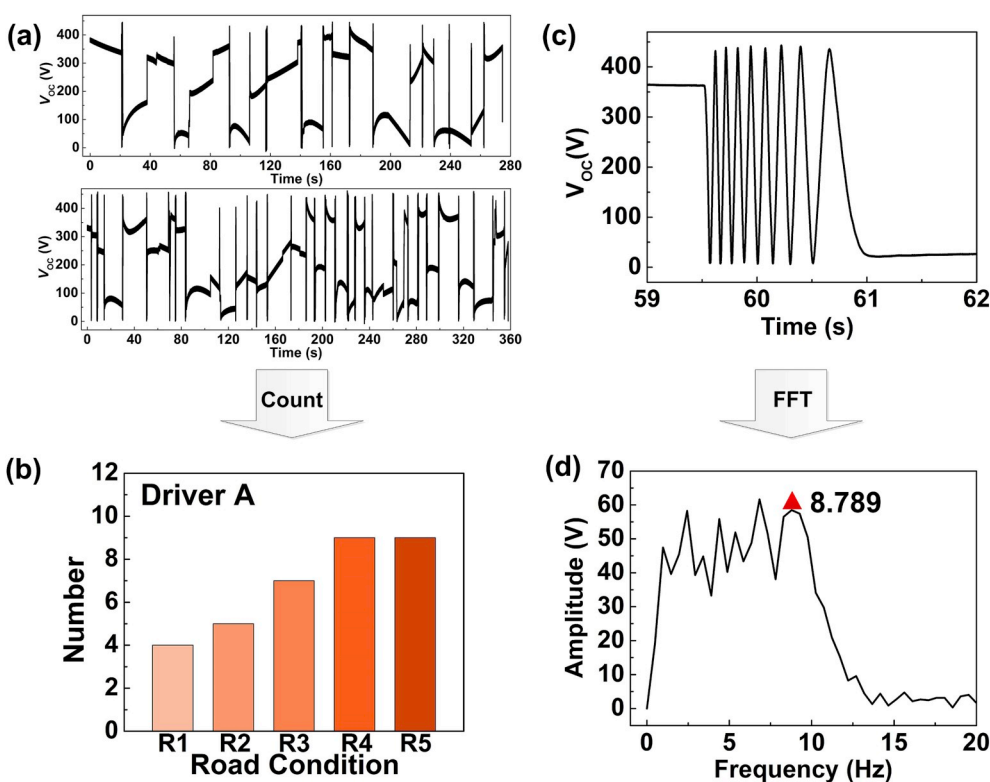


Fig. 5. Monitoring of driver habits: (a) Original signal of the Driver A; (b) the numbers of times that Driver A stepped on the accelerator and brake pedals when driving under different road conditions; (c) voltage signal of the Driver A; and (d) the frequency-domain signals.

pedals when driving under different road conditions. After a triggering, the speed of the flywheel decreases gradually owing to friction resistance. The corresponding characteristic frequency can be obtained by fast Fourier transform (FFT) of time domain signals. It is concluded from the corresponding relationship between the speed and characteristic frequency that the flywheel has the highest speed and characteristic frequency when the driver first steps on the pedal. In this, using the highest characteristic frequency to detect the driver habits is appropriate. The corresponding relationship between characteristic frequency and trigger speed is shown in Supporting Formula Equation S(7) and Fig. S6. Fig. 5d shows the frequency-domain signal obtained by FFT transformation of the original time-domain signal (Fig. 5c). The abscissa of the last peak corresponds to the highest frequency of the time-domain signal.

The reliability of the ST-TENG in monitoring driving habits was

tested. Four volunteer drivers that selected were legal and safe driving (Fig. 6a, d, g, j) were selected for the experimental study, as shown in Fig. 6. The accelerator pedal signals of the four drivers were recorded for the same road (Fig. 6b, e, h, k). It shows that each driver's total driving time and step speed were different (Fig. 6c, f, i, l). And the stepping signal and thus the stepping speed was different for each driver. It can analyses that Driver A stepped on the accelerator pedal more quickly, Drivers B and D stepped on the accelerator pedal speed more slowly, Drivers C and D stepped on the accelerator pedal fewer times than Drivers A and B. These information are valuable for monitoring driver habits.

Driver habits were investigated under different road conditions. Setting up different road conditions and letting four drivers drive from the starting point to the end point, as shown in Fig. 7a. There were five sections from low (light red) complexity to high (crimson) complexity.

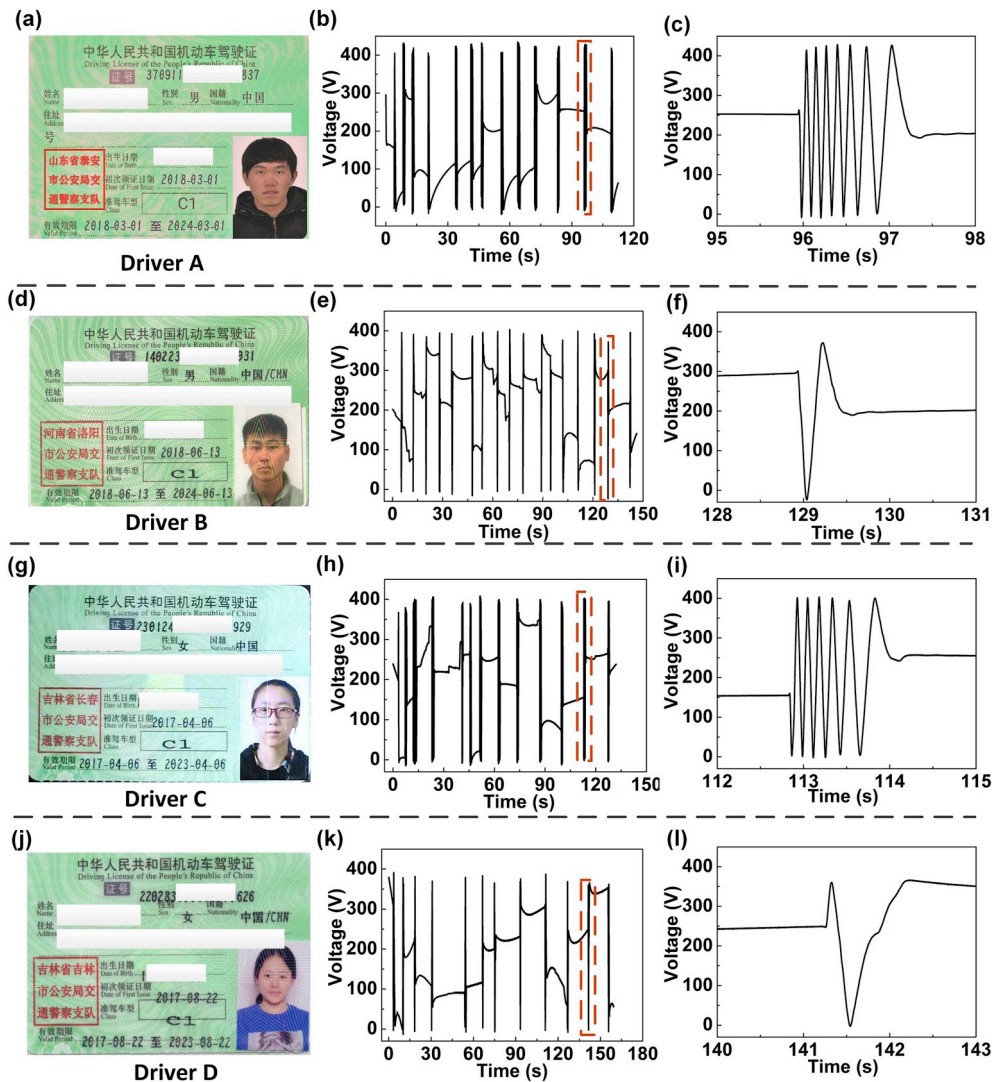


Fig. 6. Driving simulation: (a–c), (d–f), (g–i) and (j–l) driving licenses, accelerator pedal data and signal amplifications for the four drivers.

Fig. 7b and c presents times the four drivers stepped on the brake pedal and accelerator pedal under the five road conditions. Different drivers clearly have different driving habits. Driver A and B prefers to control the speed with the accelerator rather than the brake when driving in heavy traffic; under relatively low complexity road conditions, Drivers A, B and D prefer to use the accelerator to control the speed. On the whole, as the road conditions become increasingly complexity, times that four drivers step on the accelerator and brake present an upward trend in Fig. 7d, the above data analysis may reflect the road conditions. Long-term data collection may allow the prediction of the risk of traffic accidents and make an important contribution to the field of artificial intelligence driving. Three authors (Drivers E, F, and G) also participated in the text, details are presented in Figs. S6, S7 and S8.

The road sequence setting is shown in Fig. 8a. Eight traffic warning signs were set along the stretch of road to indicate a crosswalk, traffic lights, speed bumps, school, intersection, speed bumps, a crosswalk and traffic lights. Along this road sequence, four drivers drive a car from the start point to the end point. The purpose of the experiment is to study the speed at which the different drivers stepped on the brake and accelerator for the same road. Fig. 8b and c respectively show the signal frequencies of different drivers stepping on the brake pedal and accelerator pedal. Fig. 8d and e respectively present the average speed at which the four drivers stepped on the brake pedal and accelerator pedal. When the traffic light was red, the four drivers stepped on the brake pedal more

rapidly. The average speed of stepping indicates the stability of driving and may also reflect the personality of the driver. Drivers who step on a pedal rapidly may be impatient while drivers stepping slowly may have a gentler nature. The risk of traffic accidents may be predicted through long-term data collection.

4. Conclusions

A novel sweep-type triboelectric nanogenerator (ST-TENG) utilizing a single freewheel to harvest random triggering motion energy was designed for monitoring driver habits. The ST-TENG has a maximum open-circuit voltage of 400 V and maximum short-circuit current of 15 μ A. As a result, the ST-TENG can light 500 LEDs and power commercial temperature sensors through a parallel commercial capacitor and rectifier. The most important, it also can monitor driving habits, analyze road conditions after data processing and record data during driving. Through FFT transformation, we can analyze the stepping signal of driver and find that different drivers have different driving habits. This is an important breakthrough in the field of artificial intelligence driving and safe driving. The ST-TENG will be beneficial to the popularization of artificial intelligence driving. In the future, by cooperating with the machine learning and on-board intelligent driving system, transmitting real-time data to a cellphone, data of each driver can be used for connected vehicles.

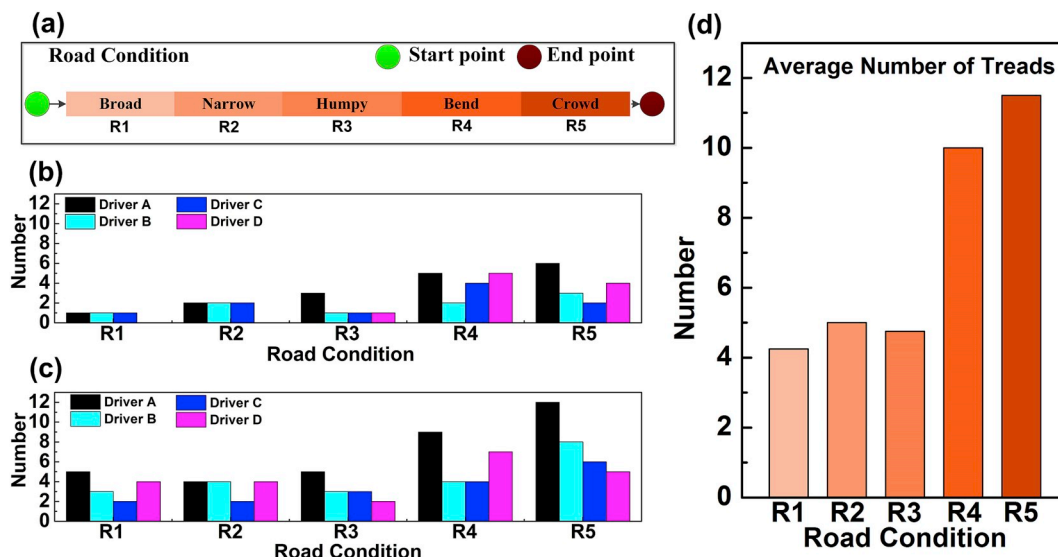


Fig. 7. Record of the number of times drivers stepped on pedals: (a) Setting of road conditions, (b) number of times the four drivers stepped on the brake under different road conditions, (c) number of times the four drivers stepped on the accelerator under different road conditions and (d) average number of times the four drivers stepped on pedals under different road conditions.

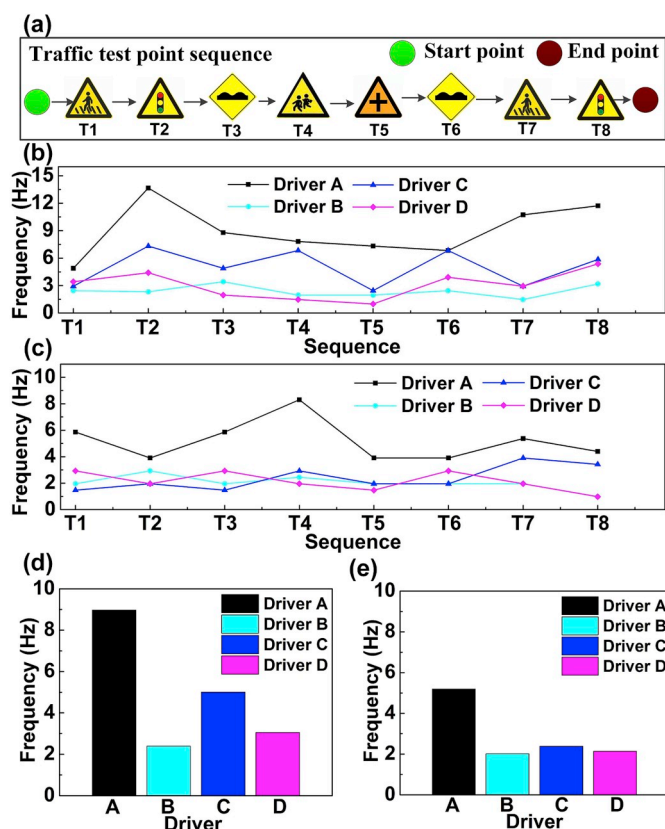


Fig. 8. (a) Road sequence in the experiment. (b) Signal frequency for drivers stepping on the brake pedal. (c) Signal frequency for drivers stepping on the accelerator pedal. (d) Average speed at which the four drivers stepped on the brake pedal. (e) Average speed at which the four drivers stepped on the accelerator pedal.

5. Experimental section

5.1. Fabrication of the ST-TENG

The sweep-type triboelectric nanogenerator (ST-TENG) has dimensions of 125 mm (length) × 95 mm (width) × 95 mm (height). The shells, flywheel and guide rail of the push rod, are made by 3D printing, the print material being polylactic acid (PLA). The single freewheel is that of a commercially available bicycle. The rotating shaft of the ST-TENG is machined by a lathe. A steel plate has the mass of 44 g, diameter of 63 mm and thickness of 1.5 mm. The flexible FEP films have a thickness of 100 μm and width of 30 mm. Ten copper electrodes with a thickness of 100 μm, width of 25 mm, and length of 30 mm are evenly distributed on the inner wall of the shells. Other information is given as supporting information.

5.2. Electrical measurement

The triggering is generated by a stepper motor (J-5718HBS401, Yisheng, China) and the ST-TENG's signal was captured by a programmable electrometer (6514, Keithley, USA) and a data acquisition system (PCI-6259, National Instruments, USA). The signal is transmitted to the computer and recorded by LabVIEW. The driving simulator is ready for testing (SiYuan SY-MNQ1).

Declaration of competing interest

We declare that we do not have any commercial or associative interest that represents a conflict of interest in connection with the work submitted.

Acknowledgment

The authors are grateful for financial support from the National Key R&D Project from the Minister of Science and Technology (2016YFA0202704), the National Key Research and Development Program of China (MB20170134), and the National Natural Science Foundation of China (grant numbers 51805109, U1737204 and 51775130).

Appendix A. Supplementary data

Supplementary data to this article can be found online at <https://doi.org/10.1016/j.nanoen.2019.104360>.

References

- [1] A. Patel, E. Krebs, L. Andrade, S. Rulisa, J. Vissoci, C. Staton, The epidemiology of road traffic injury hotspots in Kigali, Rwanda from police data, *BMC Public Health* 16 (2016) 697.
- [2] C. Tran, A. Doshi, M. Trivedi, Modeling and prediction of driver behavior by foot gesture analysis, *Comput. Vis. Image Understand.* 116 (2012) 435–445.
- [3] P. Forsman, B. Vila, R. Short, C. Mott, H. Van Dongen, Efficient driver drowsiness detection at moderate levels of drowsiness, *Accid. Anal. Prev.* 50 (2013) 341–350.
- [4] M. Lemke, Correlation between EEG and driver's actions during prolonged driving under monotonous conditions, *Accid. Anal. Prev.* 14 (1982) 7–17.
- [5] M. Lemke, Zusammenhang zwischen Fahrverhalten und hirnelektrischer Aktivität beim Führen eines Kraftfahrzeugs unter Monotoniebelastung, Verlag Nicht Ermitteltbar, 1979.
- [6] X. Zeng, J. Wang, A stochastic driver pedal behavior model incorporating road information, *IEEE Trans. Human Mach. Syst.* 47 (2017) 614–624.
- [7] J. Wang, M. Lu, K. Li, Characterization of longitudinal driving behavior by measurable parameters, *Transp. Res. Rec.* 2185 (2010) 15–23.
- [8] Q. Ji, X. Yang, Real-time eye, gaze, and face pose tracking for monitoring driver vigilance, *Real Time Imag.* 8 (2002) 357–377.
- [9] S. Wang, L. Lin, Z.L. Wang, Nanoscale triboelectric-effect-enabled energy conversion for sustainably powering portable electronics, *Nano Lett.* 12 (2012) 6339–6346.
- [10] J. Zhong, Q. Zhong, F. Fan, Y. Zhang, S. Wang, B. Hu, Z.L. Wang, J. Zhou, Finger typing driven triboelectric nanogenerator and its use for instantaneously lighting up LEDs, *Nano Energy* 2 (2013) 491–497.
- [11] Q. Tang, M. Yeh, G. Liu, S. Li, J. Chen, Y. Bai, L. Feng, M. Lai, K. Ho, H. Guo, C. Hu, Whirligig-inspired triboelectric nanogenerator with ultrahigh specific output as reliable portable instant power supply for personal health monitoring devices, *Nano Energy* 47 (2018) 74–80.
- [12] P. Wang, L. Pan, J. Wang, M. Xu, G. Dai, H. Zou, K. Dong, Z.L. Wang, An ultra-low-friction triboelectric–electromagnetic hybrid nanogenerator for rotation energy harvesting and self-powered wind speed sensor, *ACS Nano* 12 (2018) 9433–9440.
- [13] I. Tcho, S. Jeon, S. Park, W. Kim, I. Jin, J. Han, D. Kim, Y. Choi, Disk-based triboelectric nanogenerator operated by rotational force converted from linear force by a gear system, *Nano Energy* 50 (2018) 489–496.
- [14] W. Liu, L. Xu, T. Bu, H. Yang, G. Liu, W. Li, Y. Pang, C. Hu, C. Zhang, T. Cheng, Torus structured triboelectric nanogenerator array for water wave energy harvesting, *Nano Energy* 58 (2019) 499–507.
- [15] T. Cheng, Y. Li, Y. Wang, Q. Gao, T. Ma, Z.L. Wang, Triboelectric nanogenerator by integrating a cam and a movable frame for ambient mechanical energy harvesting, *Nano Energy* 60 (2019) 137–143.
- [16] J. Chen, G. Zhu, W. Yang, Q. Jing, P. Bai, Y. Yang, T. Hou, Z.L. Wang, Harmonic-resonator-based triboelectric nanogenerator as a sustainable power source and a self-powered active vibration sensor, *Adv. Mater.* 25 (2013) 6094–6099.
- [17] H. Wang, C. Jeong, M. Seo, D. Joe, J. Han, J. Yoon, K. Lee, Performance-enhanced triboelectric nanogenerator enabled by wafer-scale nanogates of multistep pattern downscaling, *Nano Energy* 35 (2017) 415–423.
- [18] F. Fan, J. Luo, W. Tang, C. Li, C. Zhang, Z. Tian, Z.L. Wang, Highly transparent and flexible triboelectric nanogenerators: performance improvements and fundamental mechanisms, *J. Mater. Chem.* 2 (2014) 13219–13225.
- [19] W. Seung, H. Yoon, T. Kim, H. Ryu, J. Kim, J. Lee, J. Lee, S. Kim, Y. Park, Y. Park, Boosting power-generating performance of triboelectric nanogenerators via artificial control of ferroelectric polarization and dielectric properties, *Adv. Energy Mater.* 7 (2016) 1600988.
- [20] Y. Yang, G. Zhu, H. Zhang, J. Chen, X. Zhong, Z. Lin, Y. Su, P. Bai, X. Wen, Z. L. Wang, Triboelectric nanogenerator for harvesting wind energy and as self-powered wind vector sensor system, *ACS Nano* 7 (2013) 9461–9468.
- [21] M. Seol, J. Woo, S. Jeon, D. Kim, S. Park, J. Hur, Y. Choi, Vertically stacked thin triboelectric nanogenerator for wind energy harvesting, *Nano Energy* 14 (2015) 201–208.
- [22] Q. Liang, X. Yan, X. Liao, Y. Zhang, Integrated multi-unit transparent triboelectric nanogenerator harvesting rain power for driving electronics, *Nano Energy* 25 (2016) 18–25.
- [23] Y. Xie, S. Wang, S. Niu, L. Lin, Q. Jing, Y. Su, Z. Wu, Z.L. Wang, Multi-layered disk triboelectric nanogenerator for harvesting hydropower, *Nano Energy* 6 (2014) 129–136.
- [24] J. Chen, J. Yang, Z. Li, X. Fan, Y. Zi, Q. Jing, H. Guo, Z. Wen, K. Pradel, S. Niu, Z. L. Wang, Networks of triboelectric nanogenerators for harvesting water wave energy: a potential approach toward blue energy, *ACS Nano* 9 (2015) 3324–3331.
- [25] L. Xu, Y. Pang, C. Zhang, T. Jiang, X. Chen, J. Luo, W. Tang, X. Cao, Z.L. Wang, Integrated triboelectric nanogenerator array based on air-driven membrane structures for water wave energy harvesting, *Nano Energy* 31 (2016) 351–358.
- [26] X. Meng, Q. Cheng, X. Jiang, Z. Fang, X. Chen, S. Li, C. Li, C. Sun, W. Wang, Z. L. Wang, Triboelectric nanogenerator as a highly sensitive self-powered sensor for driver behavior monitoring, *Nano Energy* 51 (2018) 721–727.
- [27] J. Qian, D. Kim, D. Lee, On-vehicle triboelectric nanogenerator enabled self-powered sensor for tire pressure monitoring, *Nano Energy* 49 (2018) 126–136.
- [28] H. Askari, E. Hashemi, A. Khajepour, M. Khamesee, Z.L. Wang, Towards self-powered sensing using nanogenerators for automotive systems, *Nano Energy* 53 (2018) 1003–1019.
- [29] B. Zhang, J. Chen, L. Jin, W. Deng, L. Zhang, H. Zhang, M. Zhu, W. Yang, Z. L. Wang, Rotating-disk-based hybridized electromagnetic-triboelectric nanogenerator for sustainably powering wireless traffic volume sensors, *ACS Nano* 10 (2016) 6241–6247.
- [30] Q. Jing, Y. Xie, G. Zhu, R. Han, Z.L. Wang, Self-powered thin-film motion vector sensor, *Nat. Commun.* 6 (2015) 8031.
- [31] Q. Jing, Y. Choi, M. Smith, N. Čatić, C. Ou, S. Kar-Narayan, Aerosol-jet printed fine-featured triboelectric sensors for motion sensing, *Adv. Mater. Technol.* 4 (2019) 1800328.
- [32] L. Jin, B. Zhang, L. Zhang, W. Yang, Nanogenerator as new energy technology for self-powered intelligent transportation system, *Nano Energy* 66 (2019) 104086.
- [33] H. Askari, A. Khajepour, M. Khamesee, Z.L. Wang, Embedded self-powered sensing systems for smart vehicles and intelligent transportation, *Nano Energy* 66 (2019) 104103.
- [34] L. Jin, W. Deng, Y. Su, Zhong Xu, H. Meng, B. Wang, H. Zhang, B. Zhang, L. Zhang, X. Xiao, M. Zhu, W. Yang, Self-powered wireless smart sensor based on maglev porous nanogenerator for train monitoring system, *Nano Energy* 38 (2017) 185–192.
- [35] H. Zou, Y. Zhang, L. Guo, P. Wang, X. He, G. Dai, H. Zheng, C. Chen, A. Wang, C. Xu, Z.L. Wang, Quantifying the triboelectric series, *Nat. Commun.* 10 (2019) 1427.
- [36] W. Yang, Y. Wang, Y. Li, J. Wang, T. Cheng, Z.L. Wang, Integrated flywheel and spiral spring triboelectric nanogenerator for improving energy harvesting of intermittent excitations/trigging, *Nano Energy* 66 (2019) 104104.



Zhijie Xie obtained his B.S., M.S. and Ph.D. degrees in mechanical design and theory from Harbin Institute of Technology in 2007, 2009 and 2014, respectively. He is currently a lecturer in the school of mechatronics engineering, Harbin Institute of Technology. His research interests are planetary roller screw, fault diagnosis of rotating machinery and triboelectric nanogenerators.



Zhenghui Zeng was born in Fujian province, China, in 1996. Graduated from Harbin Institute of Technology, with a BS degree in mechanical design, manufacturing and automation in 2019. He continued pursuing a Master of Engineering degree from Harbin Institute of Technology, Haerbin, China, in 2019. His research interests include soft robot and triboelectric nanogenerator.



Yuqi Wang was born in 1995 Jilin province, majored in mechatronic engineering and achieved the B.E. degree from the Changchun University of Technology in 2018. He continues pursuing a Master of Engineering degree in the same school. His research interests are environmental energy harvesting through triboelectric nanogenerators.



Weixiong Yang was born in 1996 HeBei province, majored in automotive engineering and achieved the B.E. degree from Liren College, Yanshan University in 2018. He continues pursuing a Master of Engineering degree at the Changchun University of Technology. His research interests are triboelectric nanogenerator.



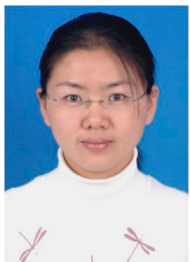
Prof. Tinghai Cheng received the B.S., M.S. and Ph.D. degrees from Harbin Institute of Technology in 2006, 2008 and 2013, respectively. He was a visiting scholar in the School of Materials Science and Engineering at Georgia Institute of Technology under the supervision of Prof. Zhong Lin (Z. L.) Wang from 2017 to 2018. His research interests are triboelectric nanogenerators, piezoelectric energy harvester, and piezoelectric actuators.



Yuhong Xu was born in 1997 Jilin province, majored in automobile service engineering the B.E. degree from the Jilin Engineering Normal University in 2019. She continues pursuing a Master of Engineering degree at the Changchun University of Technology. Her research interest focus on triboelectric nanogenerator.



Prof. Hongwei Zhao was born in Jilin, China, in 1976. He received the B.S., M.S. and Ph.D. degree in mechanical engineering from Jilin University, Changchun, China, in 2006. He was employed as a visiting researcher at Northeast University of Japan and an industry assistant researcher at the New Energy and Industrial Technology Development Organization (NEDO) in 2005. Since 2006, he has been with the School of Mechanical and Aerospace Engineering, Jilin University, where he was appointed as a teacher and is currently a professor. His current research interests include piezoelectric actuators, *in-situ* test, and precision machinery.



Xiaohui Lu was born in Jilin, China. She received the B.S. degree in mathematics and applied mathematics from Beihua University, Jilin, China, in 2004, the M.S. degree in operational research and cybernetics from the Lanzhou University of Technology, Lanzhou, China, in 2007, and the Ph.D. degree in control theory and application from Jilin University, Changchun, China, in 2013. She was a visiting scholar in School of College of Engineering at The Ohio State University under the supervision of Junmin Wang from 2017 to 2018. Her current research interests include vehicle powertrain control, model predictive control, data-driven control, and triboelectric nanogenerators.



Prof. Zhong Lin Wang received his Ph.D. from Arizona State University in physics. He now is the Hightower Chair in Materials Science and Engineering, Regents' Professor, Engineering Distinguished Professor and Director, Center for Nanostructure Characterization, at Georgia Tech. Dr. Wang has made original and innovative contributions to the synthesis, discovery, characterization and understanding of fundamental physical properties of oxide nanobelts and nanowires, as well as applications of nanowires in energy sciences, electronics, optoelectronics and biological science. His discovery and breakthroughs in developing nanogenerators established the principle and technological road map for harvesting mechanical energy from environment and biological systems for powering personal electronics. His research on self-powered nanosystems has inspired the worldwide effort in academia and industry for studying energy for micro-nano-systems, which is now a distinct disciplinary in energy research and future sensor networks. He coined and pioneered the field of piezotronics and piezophotonics by introducing piezoelectric potential gated charge transport process in fabricating new electronic and optoelectronic devices. Details can be found at: <http://www.nanoscience.gatech.edu>.